Multi-hole pressure probes

David M. Birch
May 2016

1 Introduction

Despite their comparative simplicity, multi-hole pressure probes continue to be used for the intrusive sampling of velocity components. While these sensors necessarily have a very low bandwidth (as a consequence of the length of tubing normally required to connect the probe tip to the pressure sensing elements), they have a reasonably small measurement volume (typically $\lesssim 3$ mm^3). Unlike multi-sensor hot-wire probes, however, they are temperature-insensitive and robust to the point of being nearly indestructible, and do not require frequent (time-consuming) calibration.

1.1 Principles of operation

A basic Pitot tube samples the local stagnation pressure P_0 at its central hole, and local static pressure P from holes in its side (nominally parallel to the flow). Since the probe sting may not be perfectly parallel to the flow, P is usually taken as the mean pressure from a number of holes arranged circumferentially around the probe body. Then, the local mean velocity parallel to the probe body U may be obtained from Bernoulli's equation, as

$$U = \left(\frac{2}{\rho} \left(P_0 - P \right) \right)^{1/2}, \tag{1}$$

where ρ is the fluid density, and the flow is assumed incompressible. Though (1) is formally only valid if the flow is entirely parallel to the probe axis, experiments have shown for a variety of Pitot probe tip geometries that the measured velocity is not particularly sensitive to small changes in the probe angle.

However, as the angle between the flow and the Pitot probe tip increases beyond about 10°, the pressure read by the central hole begins to decrease as a larger component of the incident flow is not brought down to stagnation conditions. While the actual pressure is a complex function of the flow angle and the probe tip geometry, for a given probe (of fixed geometry) the flow angle may be related directly to the pressure by a single function which may be obtained by calibration. Note that the effect of tip geometry upon probe effectiveness is reviewed by Chue (1975).

Consider a single, square-ended tube subjected to flow with velocity magnitude U, at some yaw angle β relative to the tube axis. If $\beta = 0°$, then the pressure P_1 recorded by the tube will be P_0. Similarly, if $\beta = 90°$, $P_1 = P_S$. For all angles within the range $0° < \beta < 90°$, then, $P_0 > P_1 > P_S$, and the relationship between P_1 and β may be expressed as

$$\beta = f_1 \left(\frac{2P_1}{\rho U^2} \right), \tag{2}$$

where f_1 is some continuous function defined for $0° \leq \beta \leq 90°$, and the pressure has been normalized against the local dynamic pressure in order to render f_1 velocity-insensitive. For $\beta < 0°$ or $\beta > 90°$, the hole will be in the wake of the body of the tube; consequently, P_1 will not yield a meaningful value for the local pressure, and f_1 will not necessarily be defined over this range.

To extend the range of measurement, we can attach two tubes side-by-side, with each ground to an angle of 45° relative to the incoming flow and 90° relative to the other; this configuration is illustrated in Figure
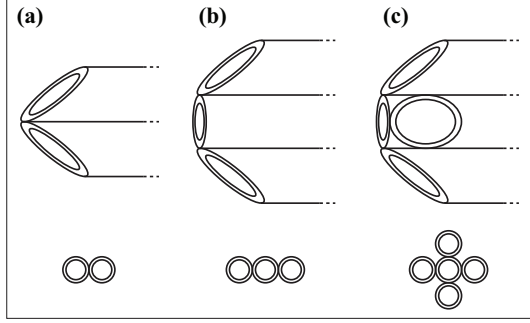
Figure 1: Geometry of common multi-hole pressure probes. (a), Two-hole yaw probe; (b) three-hole yaw-stagnation probe; (c), five-hole cruciform probe.

1(a). In this arrangement, the upper tube will be sensitive to flows between $0°$ and $45°$, while the lower tube will be sensitive to flows between $-45°$ and $0°$. The angle β may then be expressed piecewise, as

$$\beta = f_1\left(\frac{2P_1}{\rho U^2}\right) \qquad -45° < \beta < 0°$$

$$\beta = f_2\left(\frac{2P_2}{\rho U^2}\right) \qquad 0° < \beta < 45°, \tag{3}$$

where f_1 and f_2 are arbitrary functions, to be determined by calibration. This system necessarily requires *a priori* knowledge of which function to use, if a meaningful value of β is to be obtained from the set of pressures (P_1, P_2) at a given measurement station. To this end, it is useful to note that the tube to be used will always be the one with its face closest to being normal to the flow, and will therefore be registering the pressure closest to P_0 (the maximum possible value). This relationship may be used to provide an explicit definition of the ranges of the functions f_1 and f_2; (3) may equally expressed as,

$$\beta = f_1\left(\frac{2P_1}{\rho U^2}\right) \qquad P_1 > P_2$$

$$\beta = f_2\left(\frac{2P_2}{\rho U^2}\right) \qquad P_2 > P_1, \tag{4}$$

Using (4), then, one may obtain the yaw angle β of an incident flow given only the two pressures (P_1, P_2) and a measure of the local dynamic pressure. However, the velocity magnitude will remain unknown; also, the required estimate of the local dynamic pressure may not necessarily be available. In order to address this shortcoming, it is convenient to include a stagnation pressure tube in a yaw probe configuration, as illustrated in Figure 1(b). For relatively small angles, then, the central hole may be expected to yield a reasonable approximation of the local stagnation pressure. Although there is still no static pressure measurement directly available, the pressure measured by the hole *not* used in the direction measurement (and therefore reading a pressure closest to P_S) may be used as an approximation.

The concept of the three-hole yaw probe may be extended into three dimensions, by combining five tubes in a cruciform arrangement; this is commonly referred to as a *five-hole probe*, and is illustrated in Figure 1(c). The calibration space of the five-hole probe may then be expressed as,

$$\alpha = f_1\left(\frac{2P_1}{\rho U^2}\right) \qquad P_1 > P_3$$

$$\alpha = f_3\left(\frac{2P_3}{\rho U^2}\right) \qquad P_3 > P_1$$

$$\beta = f_2\left(\frac{2P_2}{\rho U^2}\right) \qquad P_2 > P_4$$

$$\beta = f_4\left(\frac{2P_4}{\rho U^2}\right) \qquad P_4 > P_2, \tag{5}$$

2

where α is the pitch angle and β is the yaw angle; the index '5' refers to the central hole, and the indices '1' through '4' indicate the peripheral holes, progressing counter-clockwise from the bottom. Furthermore, the static and stagnation pressures may be approximated as

$$
\begin{aligned}
P_0 &\approx P_5 \\
P_S &\approx \overline{P} = \frac{1}{4} \sum_{i=1}^{4} P_i.
\end{aligned}
\tag{6}
$$

The stagnation pressure is closely approximated by the pressure at the central hole, while the average of the pressures at the peripheral holes $\overline{P}$ provides an approximation of the static pressure.

There are, however, two critical shortcomings of the system of expressions given by (5) and (6): first, it is necessary to obtain four independent, piecewise functions through calibration; second, the approximations for P_0 and P_S are necessarily poor. The first problem may be addressed by redefining the functions. While the pressures at the individual holes will be sensitive to changes in flow angularity, the pressure difference between opposing holes will also be sensitive to flow angularity (although, perhaps, through a smaller range of angles). We may therefore define pitch and yaw coefficients $C_{P\alpha}$ and $C_{P\beta}$, as

$$
\begin{aligned}
C_{P\alpha} &= \frac{P_3 - P_1}{P_5 - \overline{P}} \\
C_{P\beta} &= \frac{P_4 - P_2}{P_5 - \overline{P}},
\end{aligned}
\tag{7}
$$

where we have made use of (1) and the approximations in (6) to express the dynamic pressure in terms of the available pressures. Equation (7) will also be more sensitive to the flow angle than (5), as it is a null-centric differential measure. To address the error between the approximate static and stagnation pressures used, the difference between the approximate and actual static and stagnation pressures may also be obtained through calibration, normalized against the approximate dynamic pressure and expressed as nondimensional coefficients, so that

$$
\begin{aligned}
C_{P0} &= \frac{P_5 - P_0}{P_5 - \overline{P}} \\
C_{PS} &= \frac{\overline{P} - P_S}{P_5 - \overline{P}},
\end{aligned}
\tag{8}
$$

where the values of P_0 and P_S here may be obtained elsewhere on the measurement plane (from a wind tunnel free-stream Pitot tube, for example).

In practice, then, a probe is calibrated by positioning it at a series of known angles (α, β) in a flow with a fixed, known velocity magnitude U, and recording the four coefficients $(C_{P\alpha}, C_{P\beta}, C_{P0}, C_{PS})$ at each (α, β). From this calibration data set, four independent piecewise functions may be defined, such that

$$
\begin{aligned}
\alpha &= f_\alpha(C_{P\alpha}, C_{P\beta}) \\
\beta &= f_\beta(C_{P\alpha}, C_{P\beta}) \\
C_{P0} &= f_0(C_{P\alpha}, C_{P\beta}) \\
C_{PS} &= f_S(C_{P\alpha}, C_{P\beta}).
\end{aligned}
\tag{9}
$$

Then, given any set of five pressures measured in a flow of unknown angularity and magnitude, the coefficients $C_{P\alpha}$ and $C_{P\beta}$ may be determined directly from the experimental data using (7). The flow angle (α, β) and the coefficients C_{P0} and C_{PS} may then be obtained from (9), either by interpolation or curve-fitting (see Sumner, 2002, for a comparison of these techniques). The velocity magnitude may be obtained from the interpolated values of C_{P0} and C_{PS} by re-arranging the definitions in (9) for $(P_0 - P_S)$ and substituting into (1), yielding

$$
|\mathbf{V}| = \left(\frac{2}{\rho} \left(P_5 - \overline{P} \right) \left(C_{PS} - C_{P0} + 1 \right) \right)^{1/2},
\tag{10}
$$

where $|\mathbf{V}|$ is the magnitude of the velocity vector. It is important to note here that because the static and stagnation pressure coefficients appear in (10) as a difference only, the number of required calibration functions may be reduced by defining a dynamic pressure coefficient C_{Pd}, such that

$$C_{Pd} = C_{PS} - C_{P0} = \frac{P_0 - P_S}{P_5 - \overline{P}} - 1 \tag{11}$$

The coefficient C_{Pd} may then be substituted into (10). This approach may be preferable, especially if differential pressure sensors are used as it is impossible to extract absolute pressures from the process in this case.

Though inexact, this process of reducing calibration coefficients has been well documented and is generally accepted (Treaster and Yocum, 1979). This technique may be used for flow angles up to about 30°, though the error will increase with increasing flow angle.

2 Multi-hole probes

2.1 Seven-hole probes - current practice

Seven-hole pressure probes operate on much the same principle as five-hole probes, though they do tend to be somewhat different in geometry. Seven-hole probes are fairly simple to construct, as the tubes are arranged in close-packed configuration. The tip of the probe is generally machined to form a smooth cone with a fairly steep face angle (usually 60° $\sim$ 70°, as illustrated in Figure 2). The larger number of holes tends to result in more precise measurement, while the large face angle allows the probe to measure flows of higher angularity with reasonable precision, and provides a good means of approximating the local static pressure in flows of low angularity.
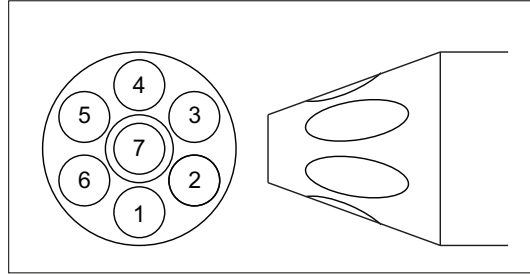

Figure 2: Typical geometry and hole numbering convention for a seven-hole pressure probe.

When operating at small flow angles, the seven-hole probe may be used in exactly the same way as a five-hole probe. The pitch and yaw angles are nondimensionalized into coefficients based on the differences between pressures on opposite sides of the probe, so that

$$\begin{aligned} C_{P\alpha} &= \frac{P_4 - P_1}{P_7 - \overline{P}} \\ C_{P\beta} &= \frac{P_5 + P_6 - P_2 - P_3}{2\left(P_7 - \overline{P}\right)}, \end{aligned} \tag{12}$$

where the hole indices are defined as shown in Figure 2, and

$$\overline{P} = \frac{1}{6} \sum_{i=1}^{6} P_i. \tag{13}$$

Note that $C_{P\alpha}$ is identical in definition to that for the five-hole probe, while $C_{P\beta}$ differs only in that the pressures on either side of the probe tip are averaged over two holes at the same horizontal position. The

4

static and stagnation pressure coefficients are likewise similarly defined, as

$$
\begin{aligned}
C_{P0} &= \frac{P_7 - P_0}{P_7 - \overline{P}} \\
C_{PS} &= \frac{\overline{P} - P_S}{P_7 - \overline{P}},
\end{aligned}
\tag{14}
$$

The flow angularity and velocities may be obtained from the calibration data as described in (9) and (10). As an example, Figure 3 shows typical values of $C_{P\alpha}$ and $C_{P\beta}$ for a seven-hole probe at small angles (so that the maximum pressure is recorded at hole 7).
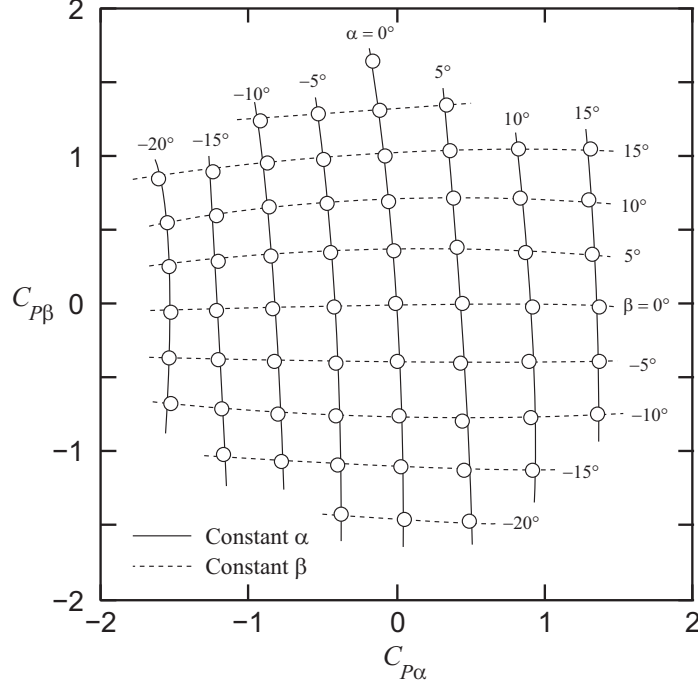

Figure 3: Coefficients of pitch and yaw for a seven-hole probe at small angles.

Because of the manner in which the coefficients in (12) and (14) are defined, these coefficients are only valid if the flow remains attached everywhere on the surface of the probe tip; typically, for a conical probe tip, this restricts the flow angularity again to about $30°$ and corresponds to cases where the maximum pressure is recorded at the centre hole. However, for the case of high angularity (where at least half of the tip of the probe is expected to be in separated flow), a new set of coefficients may be defined.

For the case of large flow angularity, it is expected that the maximum pressure P_i will be recorded at some hole i, where $i \neq 7$. Because only an angular sector of the probe tip may be used, and because the probe is axisymmetric, it is more meaningful to determine the flow angularity in terms of the cone and roll angles, θ and ϕ, in a spherical coordinate system centred at the probe tip so that

$$
\begin{aligned}
U &= |\mathbf{V}| \cos(\alpha) \cos(\beta) &= |\mathbf{V}| \cos(\theta) \\
V &= |\mathbf{V}| \sin(\alpha) &= |\mathbf{V}| \sin(\theta) \sin(\phi) \\
W &= |\mathbf{V}| \cos(\alpha) \sin(\beta) &= |\mathbf{V}| \sin(\theta) \cos(\phi),
\end{aligned}
\tag{15}
$$

The relationship between $|\mathbf{V}|$, U, V, W, α, β, θ and ϕ is illustrated in Figure 4. Then, the cone coefficient $C_{P\theta}$ and roll coefficient $C_{P\phi}$ may be defined as

$$
C_{P\theta} = \frac{P_i - P_7}{P_i - \overline{P}}
$$

$$C_{P\phi} = \frac{P_{CW} - P_{CCW}}{P_i - \overline{P}}, \tag{16}$$

where P_{CW} and P_{CCW} are the pressures recorded at the holes located adjacent to the ith hole in the clockwise and counter-clockwise directions, respectively. The coefficients of total and static pressure are then given in the same manner as (14), though recognizing that P_i now supersedes P_7 as the best available approximation of P_0, so that

$$\begin{aligned} C_{P0} &= \frac{P_i - P_0}{P_i - \overline{P}} \\ C_{PS} &= \frac{\overline{P} - P_S}{P_i - \overline{P}}. \end{aligned} \tag{17}$$

This system results in seven calibration curves; one low-angle case (for use when the maximum pressure is recorded at hole 7), and six high-angle cases (one for use in each of the cases where the maximum pressure is recorded at holes 1 through 6). This process for the calibration of seven-hole pressure probes is generally accepted, and is reviewed in detail by Zilliac (1989).
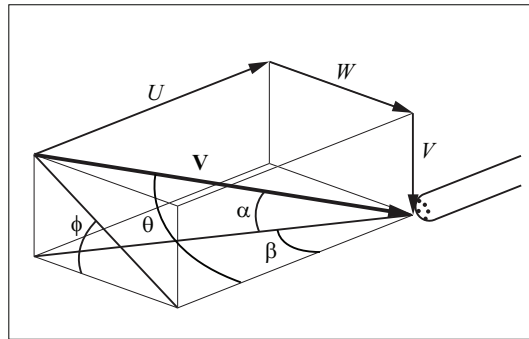

Figure 4: Graphical representation of velocities in pitch/yaw and spherical coordinate systems.

References

Chue, S. H. (1975). Pressure probes for fluid measurement. *Prog. Aerospace Sci.*, **36**(2), 147–223.

Sumner, D. (2002). A comparison of data-reduction methods for a seven-hole probe. *J. Fluids Eng.*, **124**, 523–527.

Treaster, A. L. and Yocum, A. M. (1979). The calibration and application of five-hole probes. *ISA Trans.*, **18**(3), 23–34.

Zilliac, G. G. (1989). Calibration of seven-hole pressure probes for use in fluid flows with large angularity. *NASA Technical Memorandum*, **102200**.